

Review

Polymineralic Inclusions in Megacrysts as Proxies for Kimberlite Melt Evolution—A Review

Yannick Bussweiler 

Institut für Mineralogie, Universität Münster, Corrensstraße 24, D-48149 Münster, Germany; bussweil@uni-muenster.de; Tel.: +49-251-833-6112

Received: 25 July 2019; Accepted: 29 August 2019; Published: 30 August 2019



Abstract: Polymineralic inclusions in megacrysts have been reported to occur in kimberlites worldwide. The inclusions are likely the products of early kimberlite melt(s) which invaded the pre-existing megacryst minerals at mantle depths (i.e., at pressures ranging from 4 to 6 GPa) and crystallized or quenched upon emplacement of the host kimberlite. The abundance of carbonate minerals (e.g., calcite, dolomite) and hydrous silicate minerals (e.g., phlogopite, serpentine, chlorite) within polymineralic inclusions suggests that the trapped melt was more volatile-rich than the host kimberlite now emplaced in the crust. However, the exact composition of this presumed early kimberlite melt, including the inventory of trace elements and volatiles, remains to be more narrowly constrained. For instance, one major question concerns the role of accessory alkali-halogen-phases in polymineralic inclusions, i.e., whether such phases constitute a common primary feature of kimberlite melt(s), or whether they become enriched in late-stage differentiation processes. Recent studies have shown that polymineralic inclusions react with their host minerals during ascent of the kimberlite, while being largely shielded from processes that affect the host kimberlite, e.g., the assimilation of xenoliths (mantle and crustal), degassing of volatiles, and secondary alteration. Importantly, some polymineralic inclusions within different megacryst minerals were shown to preserve fresh glass. A major conclusion of this review is that the abundance and mineralogy of polymineralic inclusions are directly influenced by the physical and chemical properties of their host minerals. When taking the different interactions with their host minerals into account, polymineralic inclusions in megacrysts can serve as useful proxies for the multi-stage origin and evolution of kimberlite melt/magma, because they can (i) reveal information about primary characteristics of the kimberlite melt, and (ii) trace the evolution of kimberlite magma on its way from the upper mantle to the crust.

Keywords: kimberlite; kimberlite melt; megacrysts; polymineralic inclusions; mantle metasomatism; decarbonation reactions

1. Introduction

Kimberlites are complex “hybrid” volcanic rocks that contain minerals of different origins, including: (i) xenocrysts from the upper mantle and crust, (ii) primary minerals crystallized (potentially at different depths) from the kimberlite melt, and (iii) secondary minerals formed during post-magmatic alteration. The multiple origins of some major mineral constituents, including olivine [1–6] and serpentine [7–11], are still debated. Due to these challenges, the composition of primary kimberlite melt remains a much sought-after problem in kimberlite petrology. Different approaches have been taken to close in on the primary composition of kimberlite, including high-pressure, high-temperature experimental studies [12–17], mass balance calculations that subtract xenocrystic components and alteration effects from natural kimberlite bulk rock compositions [18–20], and the study of melt and fluid inclusions within phenocrystic phases [21–23] or within minerals in polymict mantle breccias [24,25].

Here, the focus is on fully-crystallized melt inclusions, so-called “polymineralic inclusions”, contained within megacrysts from kimberlites. The term “megacryst” applies to mantle minerals that are >1 cm in size. Common megacryst phases are clinopyroxene, garnet, olivine, ilmenite, phlogopite, and zircon [26–28]. Based on their composition, megacrysts can be divided into a Cr-poor and a Cr-rich suite [29–31]. The origin of megacrysts themselves has long been debated. Some studies have advocated for a genetic link between a kimberlitic or “proto-kimberlitic” melt [29,32–38], whereas others considered the megacryst parental melt to be unrelated to kimberlites [26,39,40]. In the scenario that megacrysts are linked to crystallization from proto-kimberlitic melts in the lithospheric mantle, the spectrum of Cr-poor to Cr-rich megacrysts has been proposed to be a function of variable interaction with the surrounding mantle [30,41,42].

The formation of polymineralic inclusions in megacrysts has been attributed to a variety of metasomatic agents in the upper mantle, including the megacryst magma, which also crystallized the host megacrysts [43], primary or early kimberlite melt [44–46], mantle carbonatite with a subduction origin [47,48], or even diamond-forming fluids [49,50]. Here, the findings of previous studies on polymineralic inclusions in megacrysts from kimberlites are discussed. The aim of this review is to highlight the potential of polymineralic inclusions to provide new insights about kimberlite magmatism.

Polymineralic Inclusions in Megacrysts—Early Studies to Current Models of Formation

Polymineralic inclusions are fully crystallized, or crystals plus quenched melt-inclusions that are polygonal to spheroidal in shape and up to a few mm in diameter (Figure 1). They have been reported to occur in different megacryst minerals, including olivine, garnet, and ilmenite, but appear to be especially abundant within clinopyroxene megacrysts (Figure 1a, Table 1). Polymineralic inclusions are typically located where fractures or veinlets in the host megacryst converge, and are usually surrounded by regions and trails of smaller melt inclusions and fluid inclusions (Figure 2). In a recent study by Abersteiner et al. [46], the smaller melt inclusions were described as “micro-melt inclusions” (MMIs), and this term is adopted here. Polymineralic inclusions within clinopyroxene megacrysts are typically surrounded by “spongy rims” (i.e., regions where the clinopyroxene is altered and contains abundant fluid/melt inclusions), whereas polymineralic inclusions within garnets are typically lined by kelyphite (Figure 2). These features have been interpreted as textural evidence for extensive reactions between the polymineralic inclusions and their host minerals [44]. In contrast, polymineralic inclusions within olivine megacrysts were interpreted to show little evidence of this chemical interaction [45].

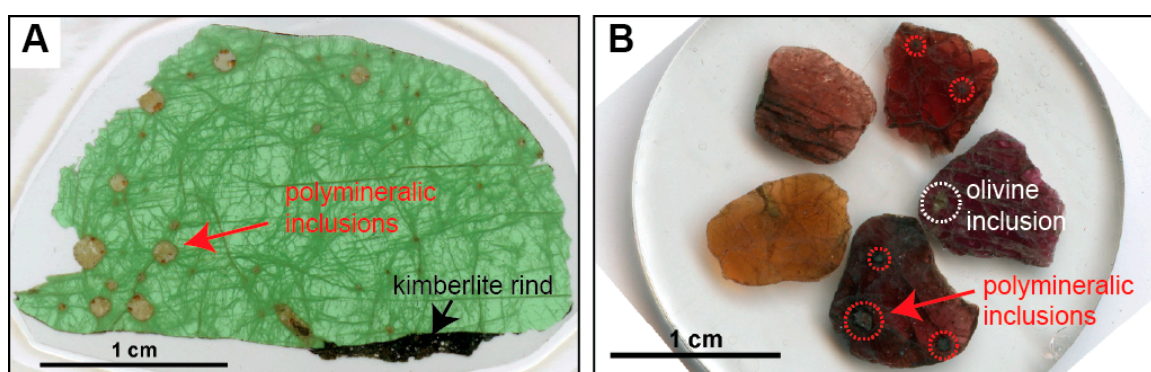


Figure 1. Photomicrographs of polymineralic inclusions within a clinopyroxene megacryst (A) and within garnet macrocrysts that possibly constitute fragments of larger megacrysts (B), from the Diavik diamond mine, Slave craton, Canada (modified after Bussweiler et al. [44]; their Figure 2). Polymineralic inclusions are typically located where fractures or veinlets in the host megacryst converge, and are surrounded by trails of smaller melt inclusions and fluid inclusions. Polymineralic inclusions are optically distinct from late-stage groundmass kimberlite (see kimberlite rind in (A)) and altered mineral inclusions (see olivine inclusion in (B)).

Table 1. Summary of previous studies on polymineralic inclusions in megacrysts from kimberlites.

References	Sample Locations	Host Minerals	Inclusion Minerals ¹	P-T Conditions of Host Minerals
Haggerty and Boyd, 1975 [51], Jakob, 1977 [52], Gurney et al., 1979 [32]	Monastery kimberlite, Kaapvaal craton, South Africa	ol	Ti-rich phl, ol, spl, ilm, grt; + sulfide-rich inclusions	~4.5 GPa
Schulze, 1985 [43]	Kentucky, USA	cpx, grt	inclusions in cpx: Ti-rich phl, srp, cc; inclusions in grt: spl, Al-rich cpx, chl	~5.5 GPa, 1050–1325 °C
van Achterbergh et al., 2002 [47]	Diavik A154N kimberlite, Slave craton, Canada	cpx	Ti-rich phl, ol, cc, Cr-spl, silicate glass, prv, sulfides	~6.2 GPa, ~1240 °C
van Achterbergh et al., 2004 [48]	<i>as above</i>	cpx	cc, silicate glass, Ti-rich phl, ol, Cr-spl, prv, sulfides (pyrite, pyrrhotite)	carbonate-rich inclusions: ~6.0 GPa, ~1235 °C, silicate-rich inclusions: 5.0 GPa ~1000 °C
Araújo et al., 2009 [49]	<i>as above</i>	cpx	cc (euhedral or as matrix), ol, mica, Mg-silicic matrix	6 GPa, 1200–1235 °C,
Pivin et al., 2009 [53]	Mbuji-Mayi & Kundelungu kimberlites, Democratic Republic of Congo	grt	phl, Ca-amphibole (K-pargasite), glass, Cr-spl	<i>no estimate</i>
Bussweiler et al., 2016 [44]	Lac de Gras kimberlites, Slave craton, Canada	cpx, grt	inclusions in cpx: phl, ol, Cr-spl/chr, srp, cc; inclusions in grt: Al-spl, Al-cpx, dol accessory minerals: ap, sulfides	~4.6 GPa, ~1015 °C
Kargin et al., 2017 [54]	Grib kimberlite, Arkhangelsk province, Russia	cpx	veinlets filled with Ti-rich phl, carbonate, srp, spl, surrounded by spongy cpx	3.6–4.7 GPa, 764–922 °C
Golovin et al., 2018 [55]	Udachnaya-East kimberlite, Siberian craton, Russia	ol in sheared peridotite	Na-carbonates, aragonite, sulphates, halides accessory minerals: ol, tetraferri-phl, mgt, djerfisherite	5.7–7.3 GPa, 1230–1360 °C
Howarth and Büttner, 2019 [45]	Monastery kimberlite, Kaapvaal craton, South Africa	ol	cc, phl, spl (low Al & Cr), prv, srp, fresh/devitrified glass; accessory minerals: ilm, ap, cpx, monticellite	4.5–6.0 GPa
Abersteiner et al., 2019 [46]	Lac de Gras & Jericho kimberlites, Slave craton, Canada; Udachnaya-East kimberlite, Siberian craton, Russia	cpx, ol	carbonate-silicate inclusions: phl, srp, cc, ol, spl (MUM), chr, ap, prv, Ni-sulfides, Ba-Sr-Na carbonates, barite alkali-carbonate-chloride-silicate inclusions: ol, phl, tetraferri-phl, shortite, pectolite, halite/sylvite, Ba-Sr carbonates, srp, K-Cl-S-bearing Mg-Fe-silicate, djerfisherite	<i>no estimate</i>

¹ Mineral abbreviations: ap = apatite, cc = calcite, chr = chromite, cpx = clinopyroxene, dol = dolomite, grt = garnet, ilm = ilmenite, mgt = magnetite, ol = olivine; prv = perovskite, phl = phlogopite, spl = spinel, srp = serpentine.

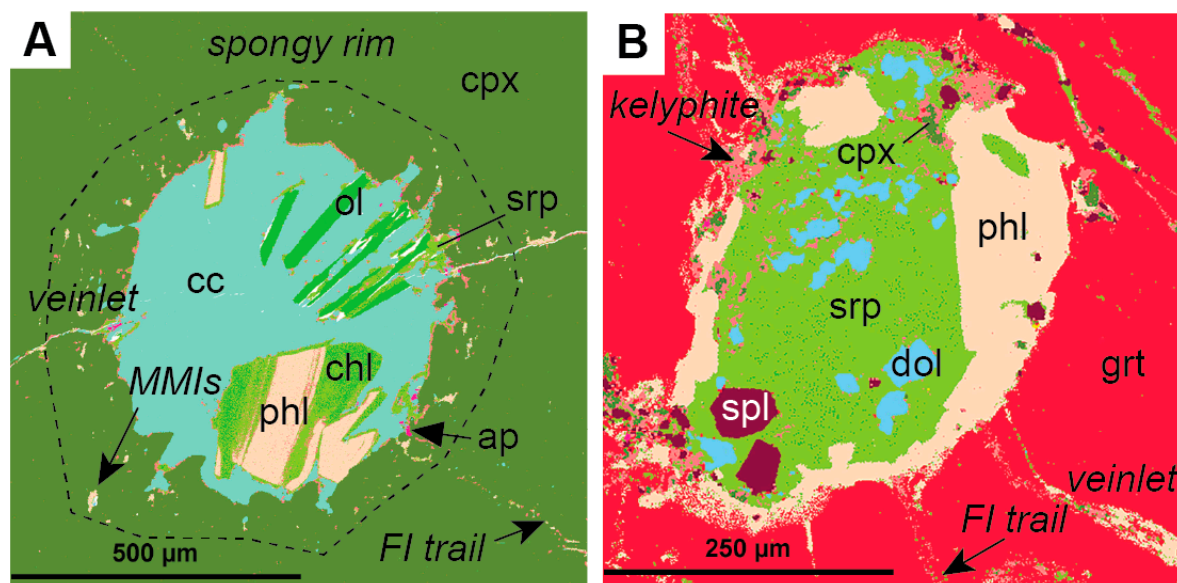


Figure 2. False-colored QEMSCAN® (Quantitative Evaluation of Minerals by Scanning Electron Microscopy) images of typical polymineralic inclusions (modified after Bussweiler et al. [44]; their Supplementary Figure 1 (A) Polymineralic inclusion within a Cr-diopside megacryst (cpx) surrounded by a spongy rim, micro-melt inclusions (MMIs), fluid inclusion (FI) trails, and veinlets. Typical inclusion phases are calcite (cc), olivine (ol), serpentine (srp), phlogopite (phl), chlorite (chl), and accessory apatite (ap); (B) Polymineralic inclusion within a Cr-pyrope megacryst (grt) surrounded by a kelyphite rim, fluid inclusion trails, and veinlets. Typical inclusion phases in addition to those observed in (A) are dolomite (dol), spinel (spl), and clinopyroxene (cpx).

Early studies on polymineralic inclusions within olivine megacrysts from the Monastery kimberlite, South Africa, favored an “entrapped liquid hypothesis”, implying that the inclusions formed from kimberlitic liquids that were present during crystallization of the host megacrysts [32,51]. Similarly, Schulze [43] proposed that the trapped liquid was also responsible for the crystallization of the host megacrysts, and concluded that the melt that formed the inclusions may have been similar to a phlogopite-bearing kimberlite, i.e., more enriched in volatiles than the host kimberlite. Importantly, Schulze [43] compared polymineralic inclusions within clinopyroxene and with those included in garnet from the same kimberlite pipe and suggested that the trapped melt was originally the same but reacted with the respective hosts to produce different mineral assemblages. Moreover, Schulze [43] first used the term “polymineralic inclusions” and already pointed out their widespread occurrence in different megacryst minerals, including ilmenite, garnet, and diopside from kimberlites in Colorado, Wyoming, and Kansas, as well as in Cr-poor megacrysts from the Jagersfontein, Kampfersdam, Frank Smith, Kao, and Camatue pipes in southern Africa. The interpretations of these early studies were adopted in the kimberlite textbook by Mitchell [27], where polymineralic inclusions are listed as evidence in support of a high-pressure phenocrystal origin of megacrysts in kimberlite.

In the following decades, research on polymineralic inclusions in megacrysts appears to have lain dormant, until van Achterbergh et al. [47] reported on melt inclusions (“globules”) within Cr-diopside megacrysts from the Diavik diamond mine in the Lac de Gras area, Slave craton (Canada). Based on detailed petrographic and geochemical observations, including trace element and isotope analysis, they suggested a link to mantle carbonatites, possibly carrying the signature of subduction fluids. In a follow-up study, van Achterbergh et al. [48] expanded on this idea to advocate for a genetic link between mantle carbonatites and kimberlites. Importantly, they found a relationship between the composition of polymineralic inclusions and the depth of origin of their host megacrysts, with deeper megacrysts hosting more carbonate-rich inclusions. Araújo et al. [49] investigated the same sample suite of Cr-diopside megacrysts from Diavik and concluded that the entire spectrum of melt inclusions

“carbonatitic” to “Mg-silicic”) is primarily a function of specifically how individual inclusions were cut, which is termed the sectioning effect. Thus, Araújo et al. [49] suggested that the melt inclusions were formed from kimberlitic melts through differentiation and wall–rock interaction. Based on trace element signatures of clinopyroxene surrounding the polymineralic inclusions, they drew a connection to diamond-forming fluids [50]. In a study on megacrysts hosted in kimberlites from the Democratic Republic of Congo, Pivin et al. [52] described “polymineral inclusions” within garnet megacrysts. They suggested that the inclusions could be the result of the destabilization of an unknown original mineral inclusion in response to a K₂O- and H₂O-rich metasomatic fluid.

More recently, Bussweiler et al. [44] revisited the Diavik megacryst samples and extended the investigation to include both clinopyroxene and garnet megacrysts from the Lac de Gras area (with samples from the Diavik and Ekati diamond mines). They concluded that polymineralic inclusions represent early kimberlite melt trapped at mantle depths which reacted extensively with the respective host minerals. Similarly, Kargin et al. [53] described veinlets filled with kimberlitic mineral assemblages within clinopyroxene megacrysts from the Grib kimberlite, Arkhangelsk province (Russia), and interpreted these as the products of intense interaction with kimberlite melt. Howarth and Büttner [45] revisited polymineralic inclusions hosted in olivine megacrysts from the Monastery kimberlite (South Africa) and described fresh silicate glass preserved within the inclusions. They also advocated for kimberlite melt entrapment at high pressure, i.e., in the subcratonic lithospheric mantle (SCLM). Based on reconstructed bulk compositions, the authors concluded that the primary kimberlite melt is carbonated silicate melt rather than carbonatite. Abersteiner et al. [46] focused on the much smaller (<5 µm) melt inclusions (i.e., MMIs) surrounding polymineralic inclusions hosted in megacrysts from Lac de Gras and Jericho kimberlites in the Slave craton (Canada), as well as from the Udachnaya kimberlite in the Siberian craton (Russia). They suggested that polymineralic inclusions, and thus early kimberlite melt, may have been enriched in alkali-halogen-phases. Golovin et al. [54] described melt inclusions preserved within sheared peridotite xenoliths from the Udachnaya-East kimberlite that are dominated by alkali-carbonates, sulphates, and halides (Table 1). Because these samples are derived from greater depths, i.e., near the base of the SCLM, they may record even deeper melts/fluids, that are potentially precursory to those producing polymineralic inclusions within megacrysts.

Based on previous studies (Table 1), polymineralic inclusions appear to be especially abundant in clinopyroxene megacrysts (also see Figure 1). This can probably be attributed to its pronounced cleavage, compared to other megacryst phases, such as olivine and garnet. The observation that polymineralic inclusions are especially abundant in megacryst suite minerals (i.e., large crystals) may be linked to the physical properties of megacrysts compared to those of the finer-grained minerals in mantle xenoliths. In case of the latter, the interaction with kimberlite melt at depth and during ascent may promote the disaggregation of xenoliths [56]. The coarser a xenolith, the sooner it will liberate its crystal cargo, which can then be invaded by the surrounding melt. Incidentally, Brett et al. [56] described similar carbonate- and phlogopite-rich inclusions of kimberlite melt in olivine macrocrysts and attributed this to “siphoning” of the melt into the liberated olivine xenocrysts during the ascent of the kimberlite.

2. Typical Mineralogy of Polymineralic Inclusions

Polymineralic inclusions are typically characterized by a groundmass composed either of carbonate (Figure 2a) or Mg-silicate/glass (Figure 2b), in which daughter crystals, often euhedral in shape, are set. The most common phase reported in polymineralic inclusions is phlogopite, which is present in all host minerals (Table 1). It often occurs as discrete, euhedral crystals (Figure 2a), or around the inclusion walls (Figure 2b). Phlogopite may be partially altered to chlorite (Figure 2a). Olivine also occurs within inclusions in all host minerals. It is often euhedral and sometimes described to have a “spinifex” texture (i.e., acicular or elongated crystals), which is indicative of fast cooling/quenching [46–48]. Olivine is typically partially serpentinized. Carbonate in polymineralic inclusions is mostly calcite (CaCO₃) of different textural varieties (i.e., euhedral to colloform), but dolomite is also observed, e.g., within

inclusions in garnet (Figure 2b). There is a clear difference in oxide minerals between polymineralic inclusions in different host minerals. Within inclusions in clinopyroxene, the oxide phase is mostly chromite (i.e., high-Cr, high-Ti), whereas within inclusions in garnet, both chromite and Cr-spinel (high-Al) occur. Within inclusions in olivine, only low-Cr, low-Al spinel occurs. Ilmenite only seems to occur within inclusions in olivine, whereas perovskite has been reported as an accessory phase within inclusions in clinopyroxene and olivine [45,46]. Al-rich clinopyroxene and dolomite only occur within polymineralic inclusions in garnet megacrysts [43,44]. Other commonly reported accessory phases in polymineralic inclusions are apatite, barite, monticellite, and amphibole (e.g., kaersutite or pargasite) (Table 1). The occurrence of phlogopite, apatite, amphibole, and carbonate minerals within the inclusions clearly indicates that the melt was volatile-bearing (i.e., CO₂, H₂O, halogens).

Based on their groundmass composition, polymineralic inclusions have been divided into carbonate-rich or silicate-rich end-members [44,48,49]. However, because mineral compositions were found to be indistinguishable across this spectrum, this is now mostly attributed to a sectioning effect (see Section 4.2). Haggerty and Boyd [51] described a separate type of sulfide-rich inclusion, which might indicate immiscibility of a sulfide-melt from the original kimberlite melt. Such pure sulfide inclusions have not been reported since (to the knowledge of the author). Yet, sulfides (i.e., pyrite/pyrrhotite, Ni-rich sulfides) are often described as accessory phases in polymineralic inclusions [44,46–48] and may constitute an important component of the original melt. It is therefore possible that Haggerty and Boyd [51] looked at a sulfide-rich region of a partially exposed polymineralic inclusion.

In addition to polymineralic inclusions, i.e., fully-crystallized and crystals plus melt-inclusions, megacrysts commonly also contain single mineral inclusions. In some cases, these may have been altered by invading fluids to produce similar mineral assemblages to those observed in polymineralic inclusions (e.g., see olivine inclusion in Figure 1b). Such altered mineral inclusions can be distinguished from polymineralic inclusions based on mineral chemistry, e.g., higher Ni contents in phases resulting from the breakdown of former olivine inclusions [44].

In summary, there is a defined relationship of the mineralogy of polymineralic inclusions with their host megacrysts. Different mineral assemblages within polymineralic inclusions may also be explained by local and regional differences in kimberlite composition, given that each kimberlite has a slightly different bulk composition [19]. However, based on previous studies that compared polymineralic inclusions in different host minerals from the same kimberlite [43,44], it appears that the host mineral exerts a strong control on which phases can form in polymineralic inclusions.

2.1. Relationship to Surrounding MMIs and Veinlets

A genetic relationship between polymineralic inclusions and the surrounding MMIs and veinlets is potentially supported by the presence of similar inclusion phases, e.g., phlogopite and calcite. However, the mechanism and timing of the formation of the surrounding MMIs, veinlets, and fluid inclusion trails is still a matter of debate. Early studies suggested that the veinlets formed outwards from the main inclusions due to sudden pressure release during eruption of the kimberlite, causing preferential liberation of volatile components [32,51]. In contrast, van Acherbergh et al. [47] surmised that the veinlets may have acted as the channel-ways along which the original melt became trapped by necking down. Bussweiler et al. [44] noted that the fluid inclusion trails are dominated by CO₂-rich inclusions, and proposed that they were produced by decarbonation reactions that occurred between the host mineral and the trapped melt (see Section 4.3.). In this scenario, the fluid inclusion trails and veinlets would form outwards due to decompression and the release of CO₂. Howarth and Büttner [45] observed that fractures around polymineralic inclusions within olivine megacrysts from the Monastery kimberlite contain partially devitrified glass, compositionally identical to the fresh residual glass within the polymineralic inclusions (see Section 2.2.), also indicating fracture formation during decompression after melt entrapment. Thus, the authors interpreted fractures and veinlets extending from the polymineralic inclusions as “expansion textures”. Abersteiner et al. [46] cautioned that many polymineralic inclusions constitute an open system, because veins that facilitated the infiltration of

kimberlite melt do not appear to have healed and sometimes connect to the surrounding kimberlite groundmass. Therefore, they suggested that MMIs may constitute more pristine samples of the trapped melt. Nevertheless, while secondary alteration cannot be ruled out, it is obvious that polymineralic inclusions are different in mineralogy and composition from typical, late-stage groundmass kimberlite, and thus preserve some characteristics of an early kimberlite melt trapped at mantle depths.

2.2. Presence of Glass in Polymineralic Inclusions

Glass within polymineralic inclusions in megacrysts has been reported in clinopyroxene megacrysts from Lac de Gras kimberlites, Slave craton (Canada) [48], in garnet megacrysts from the Mbuji-Mayi and Kundelungu kimberlites (Democratic Republic of Congo) [52], and in olivine megacrysts from the Monastery kimberlite (South Africa) [45,56]. Van Achterbergh et al. [48] noted that the silicate glass formed concentric layers alternating with carbonate-rich layers, and attributed this to unmixing during quenching (i.e., super-solidus separation). Pivin et al. [52] noted that the glass composition was too silica-rich (43–54 wt.% SiO₂) and alkali-poor (e.g., Na₂O + K₂O + CaO: 0.75–3.0 wt.%) to correspond to a typical kimberlite composition, and tentatively interpreted the inclusions to result from the breakdown of an unknown original phase which equilibrated with its host garnet during a K₂O- and H₂O-rich fluid metasomatic event. Recently, Howarth and Büttner [45] revisited glass-rich polymineralic inclusions within olivine megacrysts from the Monastery kimberlite (South Africa) and highlighted their exceptional preservation. They also reported the glass composition to be Si–Mg–Fe-rich, largely Ca–K–Ti-free, and depleted in the rare earth elements (REE). The H₂O content was estimated to be up to 10 wt.%, whereas the CO₂ content was found to be negligible. Howarth and Büttner [45] concluded that the glass component represents a quenched residual melt from which CaO, K₂O, TiO₂, CO₂, and REE were depleted during crystallization of the solid phases within the inclusions (e.g., phlogopite, calcite, perovskite, and spinel). Interestingly, the observed elevated H₂O contents would exceed those typically found within glassy melt inclusions in arc settings [57], which could be a function of (i) higher pressure of the formation of polymineralic inclusions in megacrysts, and (ii) faster ascent rates of kimberlites and thus faster quenching compared to arc magmas. Future studies could employ spectroscopic methods, e.g., Raman or Fourier-transform infrared spectroscopy (FTIR), to confidently identify the glass component within polymineralic inclusions and to quantify its volatile content.

From these previous reports, it appears that the preservation of fresh glass is more likely within olivine megacrysts. Again, this could be a function of the physical properties of the host mineral. For example, it can be noted that the average thermal conductivity is higher for forsterite (~12.3 mcal/cm sec °C) than for pyrope (~7.6 mcal/cm sec °C) and diopside (~9.8 mcal/cm sec °C) [58]. A higher thermal conductivity may enable faster quenching of the trapped melt into a glass during emplacement and cooling of the transporting kimberlite. Alternatively, inclusions in olivine may be better preserved due to less pronounced cleavage compared to clinopyroxene, shielding the inclusions more effectively from secondary alteration. In any case, the preservation of fresh glass in polymineralic inclusions is remarkable and attests to their relatively pristine nature. However, because this glass reflects the residual melt left behind after the crystallization of the inclusion assemblage, its composition needs to be integrated with those of the daughter crystals to obtain the composition of the original melt.

2.3. Origin of Serpentine in Polymineralic Inclusions

The origin of serpentine in kimberlites is still very much debated, as reflected in the recent comment and reply discussion by Fulop et al. [59,60] and Gernon et al. [61]. Whereas Fulop et al. [59,60] maintained that serpentinization in the Snap Lake kimberlite, Slave craton (Canada) is dominantly driven by deuteritic fluids, Gernon et al. [61] argued that it must be essentially completely driven by the interaction with groundwater, because the amount of released volatiles from the magma would not be large enough to cause the pervasive alteration of kimberlite. A major open question in this debate, which the study of polymineralic inclusions may help to address, is how rich in volatiles the kimberlite

magma was at mantle depths. The presence of OH-bearing minerals in kimberlites in general, and within the polymineralic inclusions in particular (see above), indicates that the melt was water-bearing.

There is evidence that some polymineralic inclusions have been affected to varying degrees by secondary alteration. For example, olivine is commonly serpentinized and phlogopite is commonly chloritized/vermiculitized (Figure 2a). In some cases, serpentine makes up the entire matrix of polymineralic inclusions in which euhedral to subhedral phases are set (Figure 2b). The origin of the fluids driving this serpentinization is still unclear. Early studies argued that fractures extending from the inclusions remained open and allowed meteoric fluids to enter [43]. However, alteration may also have been driven by deuteritic fluids from within the inclusions, i.e., residual fluids left behind after crystallization of the assemblage of daughter minerals. Bussweiler et al. [44] suggested that in addition to forming the surrounding fluid inclusions, the exsolution of a fluid phase (containing CO₂ and H₂O) may have promoted the crystallization of phlogopite, and potentially the precipitation of subsolidus serpentine within polymineralic inclusions. Howarth and Büttner [45] observed that the composition of fresh glass within polymineralic inclusions is compositionally similar to serpentine, and thus suggested that groundmass serpentine in hypabyssal kimberlites may have formed, to some extent, from the devitrification of a similar silicate melt as preserved in polymineralic inclusions. This possibility has also been suggested in some previous studies on hypabyssal kimberlites [7,62,63].

2.4. Importance of Alkali-Halogen-Phases in Polymineralic Inclusions

Abersteiner et al. [46] recently reported on alkali-carbonates and alkali-chlorides (e.g., shortite, halite/sylvite, djerfisherite) that are dominantly found within MMIs around the main polymineralic inclusions. These accessory minerals are generally small, with grain sizes <10 µm, so it is unclear how much they would contribute to the original bulk composition of polymineralic inclusions. However, because alkali-halogen-phases are highly soluble, they may have been lost due to secondary alteration or during sample preparation of polymineralic inclusions. Therefore, it is crucial to select unaltered samples and use water-free polishing agents when studying polymineralic inclusions [44,46]. In any case, the presence of alkali-carbonates and alkali-chlorides within and around polymineralic inclusions seems to suggest that the trapped melt was originally more enriched in alkalis, Cl, S, and CO₂ than the host kimberlite [46].

In this context, it may be useful to revisit the composition of other commonly observed accessory minerals in polymineralic inclusions, such as apatite and amphibole (i.e., kaersutite or pargasite). These phases are potentially more resistant to secondary alteration and may act as important hosts for halogens, e.g., F and Cl, in the mantle [64]. Phlogopite can also serve as a host for halogens, and previous studies measured moderate halogen contents in phlogopite within polymineralic inclusions (e.g., F < 0.5 wt.%, Cl < 0.1 wt.%) [44]. Van Achterbergh et al. [48], using neutron microprobe (NMP) imaging, detected areas of increased concentrations of halogens (e.g., F and Br) within polymineralic inclusions in Diavik Cr-diopsides. The analysis of phlogopite within polymineralic inclusions in olivine megacrysts from the Monastery kimberlite [45] yielded slightly higher F values (up to 1.2 wt.% with a mean of 0.51 wt.%). Abersteiner et al. [46] analyzed phlogopite within polymineralic inclusions in clinopyroxene megacrysts from different locations, including Diavik and Jericho (Slave craton, Canada), and Udachnaya (Siberian craton, Russia). Their Diavik samples yielded moderate halogen contents (F ~0.22 wt.%, Cl < 0.03 wt.%), in agreement with the findings by Bussweiler et al. [44]. In contrast, Jericho samples yielded significantly higher F values (up to 3.5 wt.% with a mean of 0.51 wt.%), whereas Udachnaya samples gave the highest mean value (~0.6 wt.% F).

In future studies, it would be interesting to test whether such elevated halogen contents in certain minerals are a general feature of polymineralic inclusions, or whether this enrichment is linked to specific locations.

3. Mineral Chemistry of Typical Phases in Polyminerale Inclusions

Bussweiler et al. [44] compared the mineral chemistry of the major mineral phases in polyminerale inclusions (e.g., olivine, phlogopite, carbonates, spinel/chromite, serpentine/chlorite) with corresponding minerals in kimberlites and, when applicable, in mantle peridotites. The two major outcomes of this comparative study were that (i) the compositions of minerals in polyminerale inclusions generally lie at the beginning of typical kimberlite differentiation trends, and (ii) the mineral chemistry is further influenced by the composition of the host. The latter is especially evident in elevated Cr concentrations (e.g., in phlogopite, Figure 3), interpreted as a function of a chemical interaction of the trapped melt with the host Cr-rich megacrysts (i.e., Cr-diopside and Cr-pyrope). New data for phlogopite in polyminerale inclusions hosted in clinopyroxene megacrysts from Jericho and Udachnaya by Abersteiner et al. [46] support this interaction with the host: phlogopite within polyminerale inclusions in megacrysts from Jericho is notably more enriched in Cr than phlogopite within the Udachnaya samples (Figure 3). This is directly reflected in the Cr contents of the host clinopyroxene megacrysts; Jericho samples contain on average ~1.2 wt.% Cr₂O₃, whereas Udachnaya samples contain only ~0.4 wt.% Cr₂O₃ [46].

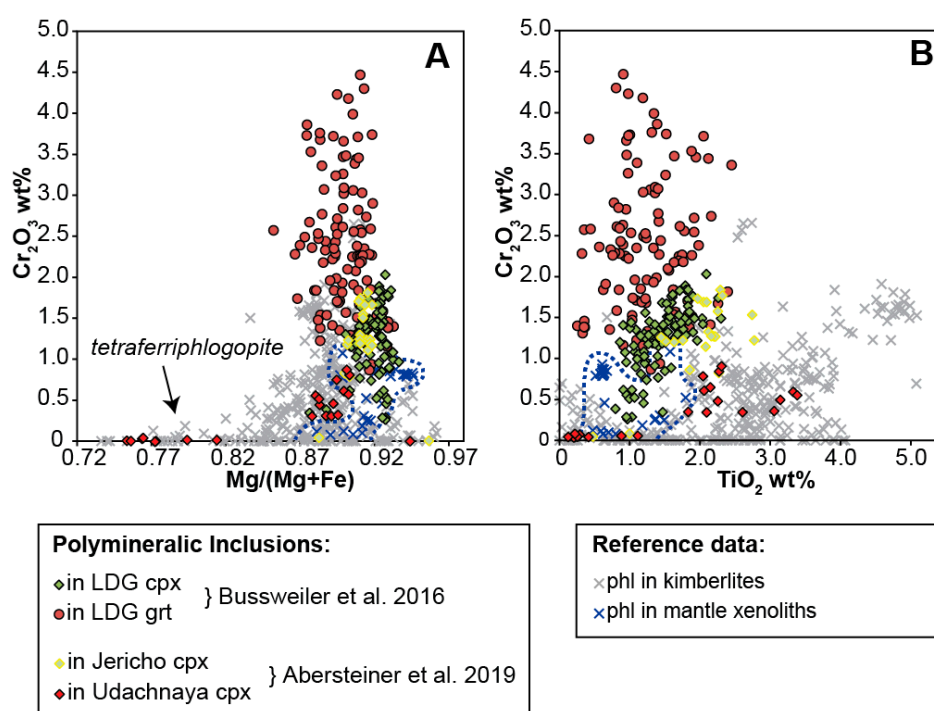


Figure 3. Compositional variation of phlogopite (A: Cr₂O₃ versus Mg/(Mg+Fe), B: Cr₂O₃ versus TiO₂) within polyminerale inclusions in clinopyroxene and garnet megacrysts from Lac de Gras (LDG) (modified after Bussweiler et al. [44]; their Figure 6), and clinopyroxene megacrysts from Jericho and Udachnaya [46]. Reference data for phlogopite in kimberlites are from Eccles et al. [65], Armstrong et al. [66], and Kopylova et al. [67]. Reference data for phlogopite in mantle xenoliths are from Menzies et al. [68] and Giuliani et al. [25].

In general, Ti-rich phlogopite appears to be a common feature of polyminerale inclusions (Table 1). Under closer inspection, however, Abersteiner et al. [46] noted that phlogopite hosted in polyminerale inclusions and MMIs can exhibit a variety of zoning patterns, including discrete internal zones characterized by decreasing TiO₂ and Al₂O₃ and increasing FeO contents (from core to rim), and thin (<10 μm) Ba-rich rims (i.e., kinoshitalite), which may be surrounded by the outermost rims of Al-free phlogopite (i.e., tetraferriphlogopite). Spinel in polyminerale inclusions can also show compositional zoning. For example, Bussweiler et al. [44] observed that chromites within polyminerale inclusions in Cr-diopsides and Cr-pyropes plot along “magmatic trend 2” [27,28], which is characterized by

Fe-enrichment prior to an increase in Ti content. This is attributed to the co-crystallization of phlogopite and olivine within the inclusions. Such complexity in mineral compositions points to fractional crystallization within the polymineralic inclusions and warrants caution when reconstructing bulk compositions (see Section 4.2.).

Interestingly, spinel within polymineralic inclusions hosted in olivine megacrysts [45] is strikingly different from spinel and chromite reported within inclusions hosted in clinopyroxene and garnet megacrysts [44]. Spinel within inclusions in olivine has low Cr₂O₃ and Al₂O₃ contents (generally <5.0 wt.% for each) and is thus more similar to magnesio-ulvöspinel-magnetite (MUM) spinels [45]. It is argued here that the absence of high-Al, high-Cr spinel within polymineralic inclusions in olivine may also be linked to the influence of the host mineral; Cr and Al are trace elements in forsterite but major components in Cr-diopside and Cr-pyrope. Ilmenite is only present within polymineralic inclusions in olivine (Table 1) and has been reported to be enriched in Mg compared to ilmenites found in the host kimberlite [51]. This could also be attributed to the high-Mg nature of the olivine host.

3.1. Trace Element Data

Trace element concentrations in minerals within polymineralic inclusions were obtained mostly for phlogopite and calcite [44,47–49], because these phases are large enough to be sampled by laser ablation inductively coupled plasma mass spectrometry (LA-ICP-MS). The trace element signatures were either compared directly to those of phlogopite and calcite in kimberlites and/or mantle peridotites [44], or combined to obtain patterns for reconstructed bulk compositions, which were then compared to patterns of whole rock kimberlites [47–49]. Figure 4 shows a compilation of trace element patterns for the Diavik sample suite, Slave craton (Canada), including the pattern of the host clinopyroxene (Cr-diopside) megacrysts, their polymineralic inclusions, and the host kimberlite (Diavik A154N). The trace element patterns of the polymineralic inclusions clearly overlap with those of the host kimberlite, supporting that they constitute trapped kimberlite melt, and not an exotic mantle carbonatite, as initially suggested by van Achterbergh et al. [47]. The host kimberlite appears to be more enriched in the elements Ba, Ti, Zr, Hf, Nb, and Ta, i.e., the high field strength elements (HFSE). This is likely due to the fact that accessory phases which are potentially enriched in HFSE (e.g., apatite, perovskite, ilmenite, amphibole, see Table 1), were not included in the reconstruction of the bulk patterns of the polymineralic inclusions.

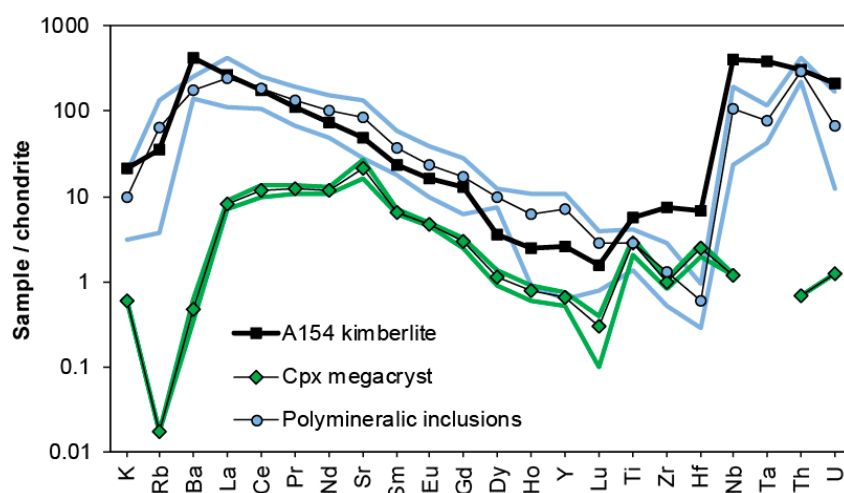


Figure 4. Chondrite-normalized (using the values by McDonough and Sun [69]) trace-element patterns of reconstructed bulk compositions of polymineralic inclusions within Diavik clinopyroxene (Cr-diopside) megacrysts compared to the pattern of the host A145N kimberlite [70]. Average concentrations for polymineralic inclusions were calculated from the data by van Achterbergh et al. [47,48] and Araújo et al. [49]. Average concentrations for clinopyroxene megacrysts were calculated from the data by van Achterbergh et al. [47,48] and Bussweiler et al. [42]. The shaded fields indicate the range between minimum and maximum values for a given element.

Araújo et al. [49] further measured trace elements in the spongy rims surrounding polymineralic inclusions in Cr-diopside megacrysts, and compared these to the signature of certain diamond-forming fluids [50]. They observed a general resemblance to the pattern of fluid inclusions in diamonds along the spectrum of saline brines to carbonatitic compositions. However, it should be noted that spongy rims contain abundant micro-inclusions of phlogopite and calcite, as well as multi-phase MMIs, which are extremely difficult to avoid during LA-ICP-MS.

Howarth and Büttner [45] presented trace element data for perovskite, calcite, phlogopite, and glass within polymineralic inclusions hosted in olivine megacrysts from the Monastery kimberlite, Kaapvaal craton (South Africa). They observed that the trace element concentrations (e.g., REE) in perovskite within polymineralic inclusions are similar to those of perovskite measured in South African kimberlites. The REE pattern of the silicate glass clearly showed REE partitioning from the melt into the solid phases, e.g., phlogopite, calcite, perovskite, and spinel, during crystallization of the inclusions [45].

In general, it can be observed that mineral compositions, in terms of major and trace elements, lie at the beginning of typical differentiation trends of kimberlite minerals. This underlines the conclusion that polymineralic inclusions represent early kimberlite melt trapped at mantle depths, not simply late-stage groundmass kimberlite.

3.2. Isotopic Data

So far, few studies have investigated the isotopic composition of phases within polymineralic inclusions. The most comprehensive study was undertaken by van Achterbergh et al. [47], who measured oxygen and strontium isotopes in the host clinopyroxene megacrysts, as well as oxygen, carbon, and strontium isotopes in calcite within the polymineralic inclusions. The $^{87}\text{Sr}/^{86}\text{Sr}$ ratio in the host clinopyroxene was ~ 0.7034 , whereas the polymineralic inclusions yielded a more radiogenic value of ~ 0.7067 . The $\delta^{18}\text{O}$ of the host clinopyroxene was $+4.0\text{‰}$ relative to standard mean ocean water (SMOW), and significantly higher for the polymineralic inclusions ($+14.2\text{‰}$ relative to SMOW). The $\delta^{13}\text{C}$ value for the polymineralic inclusion was -2.1‰ relative to Peedee belemnite (PDB). From these isotope systematics, the authors concluded that (i) the preserved isotopic disequilibrium between the host clinopyroxene and polymineralic inclusions suggests entrapment shortly before kimberlite eruption, and (ii) subducted crustal material may have been involved in the origin of the polymineralic inclusions.

Bussweiler et al. [44] measured Sr isotopes in the host clinopyroxene and garnet megacrysts, as well as in calcite in their respective polymineralic inclusions. The $^{87}\text{Sr}/^{86}\text{Sr}$ ratios of the host megacrysts were also found to be significantly lower (~ 0.7045 for clinopyroxene, ~ 0.7040 for garnet) than those of their respective polymineralic inclusions ($0.7049\text{--}0.7053$ in inclusions in clinopyroxene, $0.7061\text{--}0.7071$ in inclusions in garnet), supporting isotopic disequilibrium, in accordance with the findings of van Achterbergh et al. [47]. However, the measured $^{87}\text{Sr}/^{86}\text{Sr}$ ratios of the polymineralic inclusions still overlap with the signature of the host kimberlite, i.e., ~ 0.70619 for the Diavik A154 kimberlite [70], making an early kimberlite melt the most likely candidate for producing the polymineralic inclusions, which is also supported by the striking overlap in trace element patterns (see Figure 4). Moreover, Bussweiler et al. [44] showed that the difference in $^{87}\text{Sr}/^{86}\text{Sr}$ ratios between carbonate in polymineralic inclusion and the host megacryst was smaller for clinopyroxene than for garnet, which was taken as evidence for a stronger reaction between trapped kimberlite melt and host clinopyroxene.

Future studies could use Rb–Sr isotope systematics on phlogopite [71] to test whether the close temporal link between polymineralic inclusions and the eruption of the host kimberlite is a common feature. It may even be possible to decipher multiple kimberlite pulses at depth preceding the eruption, although compositional and isotopic heterogeneities are unlikely to be preserved for an extended time at mantle conditions. Moreover, further stable isotope data (e.g., hydrogen, oxygen, and carbon isotopes) could help to distinguish between primary (i.e., deuteric) or secondary (i.e., meteoric) origins of serpentine/chlorite in polymineralic inclusions.

4. Insights into the Evolution of Kimberlite from Mantle to Crust

Polymineralic inclusions in megacrysts can help to better understand the evolution of kimberlite melt/magma during its ascent from the upper mantle to the crust. By calculating the pressure (P) and temperature (T) of equilibration for the host megacrysts using geothermobarometry, the maximum depth of formation of polymineralic inclusions can be constrained. In order to estimate the composition of the original melt responsible for the formation of polymineralic inclusions, it is necessary to recombine the major mineral constituents according to their modal abundance, while taking into account the effects of interaction with the host, fractional crystallization (both within the inclusions and in the transporting kimberlite), and secondary alteration. Taking a comparative approach, i.e., by looking at polymineralic inclusions hosted in different megacryst phases sampled by the same kimberlite, might make it possible to deduce the “reactivity” of the original melt with different mineral phases and would help to discover common primary features (e.g., volatile content). In future studies, combining the results from different host megacrysts from different P-T conditions, but also from the same batch of kimberlite magma, could help to decipher the magma evolution of a given kimberlite. On the basis of existing studies, some general insights will be summarized here.

4.1. Depth of Formation of Polymineralic Inclusions

In order to constrain the depth of formation of polymineralic inclusions, it is helpful to know the P-T conditions under which the host megacrysts have formed. This would give a maximum depth at which entrapment of the inclusions could have occurred because, in theory, the melt could have invaded the megacrysts at any point during the ascent of the transporting kimberlite. A general challenge with estimating the P-T conditions of megacrysts is the fact that they are often monomineralic. Single-crystal thermobarometry is possible for clinopyroxene [72], but only if compositional thresholds apply that indicate equilibrium with a peridotite assemblage [73]. Therefore, previous studies have relied on megacryst samples that also contain other mineral inclusions, or inferred that the megacrysts were in equilibrium with a lherzolitic assemblage [47,48]. For Cr-rich megacrysts this assumption appears to be justified, because they are virtually indistinguishable from lherzolitic phases [29,42].

The results of previous P-T calculations for megacrysts that contain polymineralic inclusions (Table 1) indicate that the formation of megacrysts, and by extension the formation of polymineralic inclusions, occurs along a range of depths within the SCLM, generally at pressures ranging from 4 to 6 GPa and temperatures from 1050 to 1240 °C. Results for clinopyroxene megacrysts from the Grib kimberlite, Arkhangelsk province (Russia) yielded somewhat lower P-T conditions of 3.6–4.7 GPa and 764–922 °C. Older and also more recent models suggest that the formation of megacrysts could be the result of previous kimberlite pulses (i.e., proto-kimberlites) that stalled in the lithospheric mantle [30,41,42]. Once these megacrysts are sampled by a subsequent “successful” kimberlite pulse, they can become infiltrated by early kimberlite melt at depth, aided by cleavage planes or decompression cracks in the host megacrysts. As the kimberlite magma ascends, different reactions between trapped melt and host megacrysts occur along the way (see Section 4.3).

4.2. Composition of the Original Melt

Bulk compositions of the original melt(s) that formed the now fully-crystallized polymineralic inclusions are notoriously difficult to obtain. For example, Schulze [43] noted that “because of the small size and altered nature of the samples, it would be difficult to obtain meaningful modes or bulk compositions. Reaction with the garnet host has changed the bulk composition of the samples, and water at least has been added during serpentinization.” Since then, however, a range of new analytical techniques have become available, and these were used to constrain the modal and bulk composition of polymineralic inclusions. For example, van Achterbergh et al. [48] applied neutron microprobe imaging (NMP), Bussweiler et al. [44] applied Quantitative Evaluation of Minerals by Scanning Electron Microscopy (QEMSCAN[®], see Figure 2), and Howarth and Büttner [45] used large area energy

dispersive spectrometry (EDS) mapping on polymineralic inclusions. Van Achterbergh et al. [47,48] and Araújo et al. [49] calculated bulk compositions of polymineralic inclusions in terms of major and trace elements by combining EPMA with LA-ICP-MS data (see Section 3.1) for the major inclusion phases. In future studies, trace element mapping by LA-ICP-MS may prove useful in order to better constrain the trace element budget of polymineralic inclusions and to highlight potential accessory phases.

When plotting the results of these previous studies, it can be noted that the reconstructed bulk compositions of polymineralic inclusions define linear arrays in terms of the major components, i.e., in CaO–SiO₂ and MgO–SiO₂-space (Figure 5). These arrays (highlighted as dotted red arrows in Figure 5) connect the end-member compositions of calcite and olivine, both common phases within polymineralic inclusions. Thus, the observed range of compositions can primarily be attributed to a sectioning effect, i.e., whether more calcite or olivine (or other Mg–Fe-silicates) are exposed [44,49]. However, some variation may also be due to differentiation of the melt before entrapment and/or interaction with the host megacryst during or after entrapment. Howarth and Büttner [45] argued that the polymineralic inclusions that they studied within olivine megacrysts from the Monastery kimberlite were relatively pristine and did not react extensively with the host. However, when comparing their bulk compositions to the trend of previously published compositions for polymineralic inclusions, they in fact lie on a similar array, but are clustered near the composition of olivine (Figure 5). Likewise, the bulk compositions of polymineralic inclusions within garnet megacrysts by Bussweiler et al. [44] are clearly shifted towards the composition of the host garnet composition (Figure 5b). Thus, reaction with the host megacrysts needs to be taken into account when evaluating the bulk composition of polymineralic inclusions.

When comparing the reconstructed bulk compositions of polymineralic inclusions with those of possible primary kimberlite melts produced in high-pressure, high-temperature experiments [12–16,74], it can be noted that the experimental melts mostly lie on the lower-SiO₂ side relative to the polymineralic inclusion array (Figure 5). Importantly, there is good overlap with low-degree melts produced at 7 GPa and 1400 °C in recent experimental studies [16,75]. The same holds true for the range of reconstructed primary compositions for South African kimberlites by Soltys et al. [20], which overlap the compositional array defined by the polymineralic inclusions on the lower-SiO₂ side (Figure 5). Thus, primary kimberlite melt compositions, i.e., from within the experimental melt fields, can theoretically be projected onto the polymineralic inclusion arrays by reaction with the host megacrysts, e.g., clinopyroxene or garnet. Reaction with/dissolution of orthopyroxene and olivine may play a role as well. However, experimental studies have shown that the dissolution of orthopyroxene in ascending carbonate-rich melts is not effective until pressures of <3.5 GPa [76] and that decarbonation does not occur until depths of <100 km [77]. Yet, the dissolution of orthopyroxene is also a function of the primary melt composition, and other experimental studies suggested that in a Na₂CO₃ melt this process would occur sooner and could result in the formation of a homogeneous silicate–carbonate melt at 5.0 GPa and 1200 °C [78].

In contrast to the experimental melts shown in Figure 5, melts produced from the melting of Udachnaya-East kimberlite (Siberian craton, Russia) [79,80] generally yield significantly lower SiO₂ and MgO contents (both <12 wt.%), and higher CaO (up to ~28 wt.%) and Na₂O contents (up to ~10 wt.%). If instead these compositions represent the primary kimberlite melt, a higher degree of assimilation of mantle minerals would be required to produce the melt(s) which formed the polymineralic inclusions.

In addition to the major and trace elements discussed above, the common presence of accessory sulfides and sulphates within polymineralic inclusions (Table 1) suggests that early kimberlite melt may contain a significant sulfur component. The reconstructed bulk composition (“bulk globule”) by van Achterbergh et al., 2004, indicates that the S content may be ~0.5 wt.%.

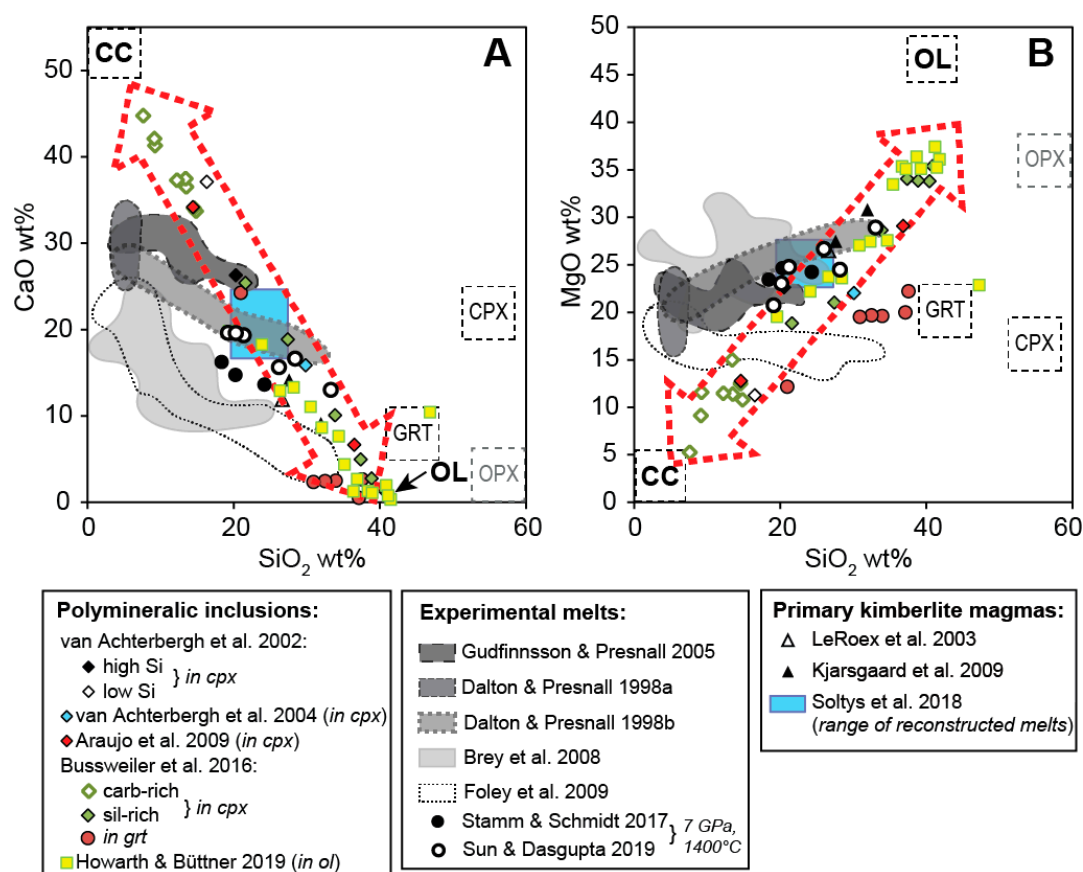


Figure 5. Reconstructed bulk compositions of polymineralic inclusions from various studies (see legend) plotted together with experimental melts (shaded fields), estimates of primary kimberlite magmas from natural kimberlites (triangles), and end-member compositions of calcite (cc), olivine (ol), garnet (grt), clinopyroxene (cpx), and orthopyroxene (opx) (modified after Bussweiler et al. [44]; their Figure 12). The blue rectangle represents the range of reconstructed primary compositions for South African kimberlites by Soltys et al. [20]. The CaO versus SiO₂ plot (A) and MgO versus SiO₂ plot (B) show that reconstructed bulk compositions of polymineralic inclusions mostly define compositional arrays (dotted red arrows) between the end-members cc and ol, which is probably a function of a sectioning effect. Possible primary compositions, i.e., from within the experimental melt fields, can be projected onto the polymineralic inclusion arrays by reaction with the host megacrysts, e.g., clinopyroxene or garnet. Reaction with/dissolution of orthopyroxene and olivine may play a role as well.

4.3. Differentiation of Kimberlite Melt and Interaction with Megacryst Hosts during Ascent

The picture that emerges from the study of polymineralic inclusions is that of a multi-stage origin for kimberlites and their high-pressure mineral constituents, i.e., megacrysts. Kimberlites form in multiple pulses, stall in the upper mantle, and form megacrysts at a range of depths. Subsequent kimberlite pulses can entrain these megacrysts and the transporting melt can infiltrate them to form melt inclusions, possibly at various stages during the ascent of the host magma, which crystallize upon kimberlite emplacement to form polymineralic inclusions. Interestingly, van Achterbergh et al. [48] initially suggested that polymineralic inclusions in deeper samples are more carbonate-rich, whereas polymineralic inclusions in shallower samples are more silicate-rich. This could indicate progressive differentiation of the kimberlite melt, e.g., by reaction/dissolution of mantle minerals. However, the different end-members (carbonate-rich versus silicate-rich) were later attributed to sectioning effects because the mineral compositions are essentially identical [44,49]. A more rigorous investigation of a suite of megacryst minerals and their polymineralic inclusions, which combines geothermobarometry with careful petrographic observations, could test this hypothesis.

Once the potentially variably differentiated melt is trapped in the host megacrysts, it undergoes different reactions with the different host minerals. For example, Bussweiler et al. [44] showed that polymineralic inclusions within Cr-diopsides record the decarbonation reaction of dolomitic melt + diopside \rightarrow forsterite + calcite + CO₂. Similarly, kelyphite around polymineralic inclusions within garnet results from decompression reactions with the trapped kimberlite melt, which has previously been proposed for kelyphite rims commonly observed around garnet xenocrysts [81]. In contrast, Howarth and Büttner [45] found little textural or chemical evidence for interaction with the trapped melt and host olivine megacrysts. This could suggest that olivine is a more “inert” container for early kimberlite melt than, for example, clinopyroxene and garnet, which would be in agreement with the abundance of olivine xenocrysts in kimberlite [1–6]. For the polymineralic inclusions in olivine megacrysts, the differentiation of the melt seems to be mainly controlled by the crystallization of phases present within the polymineralic inclusions, e.g., perovskite, phlogopite, calcite, and spinel [45]. Nevertheless, the distribution of reconstructed bulk compositions of polymineralic inclusions in olivine (Figure 5) seems to suggest that some reaction between the trapped melt and the host olivine has occurred. Upon emplacement of the kimberlite, polymineralic inclusions are fully crystallized or quenched to a glass, and in most cases shielded within their host megacrysts from degassing and secondary alteration processes that affect the surrounding kimberlite. In general, the crystallization sequence of polymineralic inclusions is similar to that of typical Group I kimberlites (e.g., [82]). After melt entrapment and reaction with the host, olivine and phlogopite seem to crystallize first (as indicated by their large crystal sizes and euhedral shapes), followed by the crystallization of spinel and accessory phases (e.g., apatite, perovskite, barite), and crystallization/quenching of a groundmass, which resembles the ‘mesostasis’ of carbonate and serpentine commonly observed in kimberlites. Prominent exceptions to this crystallization sequence are minerals such as Al-rich clinopyroxene, Al-rich spinel, and euhedral dolomite (e.g., within polymineralic inclusions in garnet), which are typically absent from kimberlites. Here, these phases are interpreted to result from the interaction with the host megacrysts.

5. Conclusions and Outlook

Polymineralic inclusions within megacrysts from kimberlites likely represent kimberlite melt trapped at mantle depths which reacted with the host megacrysts during kimberlite ascent and fully crystallized or quenched upon emplacement of the transporting kimberlite. Such inclusions have now been described from different locations around the globe, including the Slave craton (Canada), the North American craton (USA), the Siberian craton (Russia), the East European craton (Russia), and the Kaapvaal craton (South Africa). By bringing the evidence from different locations together, it appears that the host megacrysts exert a strong control on inclusion mineralogy and mineral chemistry. From this observation, it may be possible to converge on a common composition, which is most likely to represent early kimberlite melt (although different geochemical flavors are to be expected for different kimberlite occurrences). Open questions remain concerning the nature of alkali-halogen-phases within polymineralic inclusions: Are they commonly lost during secondary alteration and/or sample preparation? Are they a primary feature of kimberlite melt, or do they become enriched in late-stage differentiation processes? In this context, more measurements of halogen concentrations in typical phases within polymineralic inclusions would be useful. Further trace element and isotopic studies on polymineralic inclusions are needed to pinpoint the origin of different inclusion phases, e.g., serpentine, and eventually the source(s) and composition(s) of the primary kimberlite melt. Finally, there are some similarities between the polymineralic inclusions described here and multi-phase inclusions in fibrous diamonds [83]. The latter also commonly contain phlogopite and carbonate as daughter minerals, and there also is a saline end-member of high-density fluid (HDF) inclusions [84,85]. A possible link between HDF inclusions in diamonds and polymineralic inclusions in megacrysts remains to be investigated in future studies.

Funding: The author was funded through an EU Marie Skłodowska-Curie Fellowship (Project ID 746518) at the University of Münster.

Acknowledgments: The author would like to thank Igor Sharygin for the invitation to contribute to the Minerals special issue “Minerals of Kimberlites”. The manuscript greatly benefitted from discussions with Bruce Kjarsgaard, Graham Pearson, and Stephan Klemme. Two anonymous reviewers and Igor Shaygin are thanked for constructive comments that greatly improved the manuscript. Donna Zheng is thanked for efficient editorial handling.

Conflicts of Interest: The author declares no conflict of interest.

References

1. Kamenetsky, V.S.; Kamenetsky, M.B.; Sobolev, A.V.; Golovin, A.V.; Demouchy, S.; Faure, K.; Sharygin, V.V.; Kuzmin, D.V. Olivine in the Udachnaya-East Kimberlite (Yakutia, Russia): Types, Compositions and Origins. *J. Petrol.* **2008**, *49*, 823–839. [[CrossRef](#)]
2. Brett, R.C.; Russell, J.K.; Moss, S. Origin of olivine in kimberlite: Phenocryst or impostor? *Lithos* **2009**, *112*, 201–212. [[CrossRef](#)]
3. Pilbeam, L.H.; Nielsen, T.F.D.; Waight, T.E. Digestion Fractional Crystallization (DFC): An Important Process in the Genesis of Kimberlites. Evidence from Olivine in the Majuagaa Kimberlite, Southern West Greenland. *J. Petrol.* **2013**, *54*, 1399–1425. [[CrossRef](#)]
4. Bussweiler, Y.; Foley, S.F.; Prelević, D.; Jacob, D.E. The olivine macrocryst problem: New insights from minor and trace element compositions of olivine from Lac de Gras kimberlites, Canada. *Lithos* **2015**, *220–223*, 238–252. [[CrossRef](#)]
5. Bussweiler, Y.; Brey, G.P.; Pearson, D.G.; Stachel, T.; Stern, R.A.; Hardman, M.F.; Kjarsgaard, B.A.; Jackson, S.E. The aluminum-in-olivine thermometer for mantle peridotites—Experimental versus empirical calibration and potential applications. *Lithos* **2017**, *272–273*, 301–314. [[CrossRef](#)]
6. Giuliani, A. Insights into kimberlite petrogenesis and mantle metasomatism from a review of the compositional zoning of olivine in kimberlites worldwide. *Lithos* **2018**, *312–313*, 322–342. [[CrossRef](#)]
7. Skinner, E.M.W.; Marsh, J.S. Distinct kimberlite pipe classes with contrasting eruption processes. *Lithos* **2004**, *76*, 183–200. [[CrossRef](#)]
8. Mitchell, R.H. Petrology of hypabyssal kimberlites: Relevance to primary magma compositions. *J. Volcanol. Geotherm. Res.* **2008**, *174*, 1–8. [[CrossRef](#)]
9. Mitchell, R.H. Paragenesis and Oxygen Isotopic Studies of Serpentine in Kimberlite. *Proc. Int. Kimberl. Conf.* **2013**, *1*, 1–12.
10. Stripp, G.R.; Field, M.; Schumacher, J.C.; Sparks, R.S.J.; Cressey, G. Post-emplacement serpentinization and related hydrothermal metamorphism in a kimberlite from Venetia, South Africa. *J. Metamorph. Geol.* **2006**, *24*, 515–534. [[CrossRef](#)]
11. Sparks, R.S.J. Kimberlite Volcanism. *Annu. Rev. Earth Planet. Sci.* **2013**, *41*, 497–528. [[CrossRef](#)]
12. Dalton, J.A.; Presnall, D.C. The Continuum of Primary Carbonatitic–Kimberlitic Melt Compositions in Equilibrium with Lherzolite: Data from at 6 GPa. *J. Petrol.* **1998**, *39*, 1953–1964.
13. Gudfinnsson, G.H.; Presnall, D.C. Continuous gradations among primary carbonatitic, kimberlitic, melilititic, basaltic, picritic, and komatiitic melts in equilibrium with garnet lherzolite at 3–8 GPa. *J. Petrol.* **2005**, *46*, 1645–1659. [[CrossRef](#)]
14. Brey, G.P.; Bulatov, V.K.; Gurnis, A.V.; Lahaye, Y. Experimental Melting of Carbonated Peridotite at 6–10 GPa. *J. Petrol.* **2008**, *49*, 797–821. [[CrossRef](#)]
15. Foley, S.F.; Yaxley, G.M.; Rosenthal, A.; Buhre, S.; Kiseeva, E.S.; Rapp, R.P.; Jacob, D.E. The composition of near-solidus melts of peridotite in the presence of CO₂ and H₂O between 40 and 60 kbar. *Lithos* **2009**, *112*, 274–283. [[CrossRef](#)]
16. Stamm, N.; Schmidt, M.W. Asthenospheric kimberlites: Volatile contents and bulk compositions at 7 GPa. *Earth Planet. Sci. Lett.* **2017**, *474*, 309–321.
17. Gervasoni, F.; Klemme, S.; Rohrbach, A.; Grützner, T.; Berndt, J. Experimental constraints on mantle metasomatism caused by silicate and carbonate melts. *Lithos* **2017**, *282–283*, 173–186. [[CrossRef](#)]
18. Le Roex, A.P.; Bell, D.R.; Davis, P. Petrogenesis of Group I Kimberlites from Kimberley, South Africa: Evidence from Bulk-rock Geochemistry. *J. Petrol.* **2003**, *44*, 2261–2286. [[CrossRef](#)]

19. Kjarsgaard, B.A.; Pearson, D.G.; Tappe, S.; Nowell, G.M.; Dowall, D.P. Geochemistry of hypabyssal kimberlites from Lac de Gras, Canada: Comparisons to a global database and applications to the parent magma problem. *Lithos* **2009**, *112*, 236–248. [[CrossRef](#)]
20. Soltys, A.; Giuliani, A.; Phillips, D. A new approach to reconstructing the composition and evolution of kimberlite melts: A case study of the archetypal Bultfontein kimberlite (Kimberley, South Africa). *Lithos* **2018**, *304–307*, 1–15. [[CrossRef](#)]
21. Golovin, A.V.; Sharygin, V.V.; Pokhilenko, N.P. Melt inclusions in olivine phenocrysts in unaltered kimberlites from the Udachnaya-East pipe, Yakutia: Some aspects of kimberlite magma evolution during late crystallization stages. *Petrology* **2007**, *15*, 168–183. [[CrossRef](#)]
22. Kamenetsky, V.S.; Grütter, H.; Kamenetsky, M.B.; Gömann, K. Parental carbonatitic melt of the Koala kimberlite (Canada): Constraints from melt inclusions in olivine and Cr-spinel, and groundmass carbonate. *Chem. Geol.* **2013**, *353*, 96–111. [[CrossRef](#)]
23. Abersteiner, A.; Kamenetsky, V.S.; Kamenetsky, M.; Goemann, K.; Ehrig, K.; Rodemann, T. Significance of halogens (F, Cl) in kimberlite melts: Insights from mineralogy and melt inclusions in the Roger pipe (Ekati, Canada). *Chem. Geol.* **2018**, *478*, 148–163. [[CrossRef](#)]
24. Giuliani, A.; Kamenetsky, V.S.; Phillips, D.; Kendrick, M.A.; Wyatt, B.A.; Goemann, K. Nature of alkali-carbonate fluids in the sub-continental lithospheric mantle. *Geology* **2012**, *40*, 967–970. [[CrossRef](#)]
25. Giuliani, A.; Phillips, D.; Kamenetsky, V.S.; Kendrick, M.A.; Wyatt, B.A.; Goemann, K.; Hutchinson, G. Petrogenesis of Mantle Polymict Breccias: Insights into Mantle Processes Coeval with Kimberlite Magmatism. *J. Petrol.* **2014**, *55*, 831–858. [[CrossRef](#)]
26. Nixon, P.H.; Boyd, F.R. The Discrete Nodule Association in Kimberlites from Northern Lesotho. In *Lesotho kimberlites. Maseru*; Lesotho National Development Corporation: Maseru, Lesotho, 1973; pp. 67–75.
27. Mitchell, R.H. *Kimberlites: Mineralogy, Geochemistry and Petrology*; Plenum Press: New York, NY, USA, 1986.
28. Mitchell, R.H. *Kimberlites, Orangeites, and Related Rocks*; Plenum Press: New York, NY, USA, 1995.
29. Eggler, D.H.; McCallum, M.E.; Smith, C.B. Megacryst assemblages in kimberlite from northern Colorado and southern Wyoming: Petrology, geothermometry-barometry and areal distribution. *Mantle Sample Incl. Kimberl. Other Volcan.* **1979**, *16*, 213–226.
30. Harte, B. Mantle peridotites and processes the kimberlite sample. In *Continental Basalt and Mantle Xenoliths*; Hawkesworth, C.J., Norry, M.J., Eds.; Shiva: Nantwich, UK, 1983; pp. 46–91.
31. Boyd, F.; Dawson, J.; Smith, J. Granny Smith diopside megacrysts from the kimberlites of the Kimberley area and Jagersfontein, South Africa. *Geochim. Cosmochim. Acta* **1984**, *48*, 381–384. [[CrossRef](#)]
32. Gurney, J.J.; Jakob, W.R.O.; Dawson, J.B. Megacrysts from the Monastery Kimberlite Pipe, South Africa. In *The Mantle Sample: Inclusions in Kimberlites and Other Volcanics*; American Geophysical Union: Washington, DC, USA, 1979; Volume 16, pp. 227–243.
33. Garrison, J.R.; Taylor, L.A. Megacrysts and xenoliths in kimberlite, Elliott County, Kentucky: A mantle sample from beneath the Permian Appalachian Plateau. *Contrib. Mineral. Petrol.* **1980**, *75*, 27–42. [[CrossRef](#)]
34. Harte, B.; Gurney, J.J. The Mode of Formation of Chromium-Poor Megacryst Suites from Kimberlites. *J. Geol.* **1981**, *89*, 749–753. [[CrossRef](#)]
35. Schulze, D.J. Cr-Poor Megacrysts from the Hamilton Branch Kimberlite, Elliott County, Kentucky. *Dev. Petrol.* **1984**, *11*, 97–108.
36. Kostrovitsky, S.I.; Malkovets, V.G.; Verichev, E.M.; Garanin, V.K.; Suvorova, L.V. Megacrysts from the Grib kimberlite pipe (Arkhangelsk Province, Russia). *Lithos* **2004**, *77*, 511–523. [[CrossRef](#)]
37. Moore, A.; Belousova, E. Crystallization of Cr-poor and Cr-rich megacryst suites from the host kimberlite magma: Implications for mantle structure and the generation of kimberlite magmas. *Contrib. Mineral. Petrol.* **2005**, *149*, 462–481. [[CrossRef](#)]
38. Kopylova, M.G.; Nowell, G.M.; Pearson, D.G.; Markovic, G. Crystallization of megacrysts from protokimberlitic fluids: Geochemical evidence from high-Cr megacrysts in the Jericho kimberlite. *Lithos* **2009**, *112*, 284–295. [[CrossRef](#)]
39. Hops, J.J.; Gurney, J.J.; Harte, B. The jagersfontein Cr-poor megacryst suite—towards a model for megacryst petrogenesis. *J. Volcanol. Geotherm. Res.* **1992**, *50*, 143–160. [[CrossRef](#)]
40. Davies, G.; Spriggs, A.; Nixon, P. A non-cognate origin for the Gibeon kimberlite megacryst suite, Namibia: Implications for the origin of Namibian kimberlites. *J. Petrol.* **2001**, *42*, 159–172. [[CrossRef](#)]

41. Harte, B.; Hunter, R.H.; Kinny, P.D. Melt geometry, movement and crystallization, in relation to mantle dykes, veins and metasomatism. *Phil. Trans. R. Soc. Lond.* **1993**, *342*, 1–21.
42. Bussweiler, Y.; Pearson, D.G.; Stachel, T.; Kjarsgaard, B.A. Cr-rich Megacrysts of Clinopyroxene and Garnet from Lac de Gras Kimberlites, Slave Craton, Canada—implications for the Origin of Clinopyroxene and Garnet in Cratonic Peridotites. *Mineral. Petrol.* **2018**, *11*, 4477.
43. Schulze, D. Evidence for primary kimberlitic liquids in megacrysts from kimberlites in Kentucky, USA. *J. Geol.* **1985**, *93*, 75–79. [[CrossRef](#)]
44. Bussweiler, Y.; Stone, R.S.; Pearson, D.G.; Luth, R.W.; Stachel, T.; Kjarsgaard, B.A.; Menzies, A. The evolution of calcite-bearing kimberlites by melt-rock reaction: Evidence from polymineralic inclusions within clinopyroxene and garnet megacrysts from Lac de Gras kimberlites, Canada. *Contrib. to Mineral. Petrol.* **2016**, *171*, 65. [[CrossRef](#)]
45. Howarth, G.H.; Büttner, S.H. New constraints on archetypal South African kimberlite petrogenesis from quenched glass-rich melt inclusions in olivine megacrysts. *Gondwana Res.* **2019**, *68*, 116–126. [[CrossRef](#)]
46. Abersteiner, A.; Kamenetsky, V.S.; Goemann, K.; Golovin, A.V.; Sharygin, I.S.; Pearson, D.G.; Kamenetsky, M.; Gornova, M.A. Polymineralic inclusions in kimberlite-hosted megacrysts: Implications for kimberlite melt evolution. *Lithos* **2019**, 336–337, 310–325. [[CrossRef](#)]
47. van Achterbergh, E.; Griffin, W.L.; Ryan, C.G.; O'Reilly, S.Y.; Pearson, N.J.; Kivi, K.; Doyle, B.J. Subduction signature for quenched carbonatites from the deep lithosphere. *Geology* **2002**, *30*, 743–746. [[CrossRef](#)]
48. van Achterbergh, E.; Griffin, W.L.; Ryan, C.G.; O'Reilly, S.Y.; Pearson, N.J.; Kivi, K.; Doyle, B.J. Melt inclusions from the deep Slave lithosphere: Implications for the origin and evolution of mantle-derived carbonatite and kimberlite. *Lithos* **2004**, *76*, 461–474. [[CrossRef](#)]
49. Araújo, D.P.; Griffin, W.L.; O'Reilly, S.Y. Mantle melts, metasomatism and diamond formation: Insights from melt inclusions in xenoliths from Diavik, Slave Craton. *Lithos* **2009**, *112*, 675–682. [[CrossRef](#)]
50. Araújo, D.P.; Griffin, W.L.; O'Reilly, S.Y.; Grant, K.J.; Ireland, T.; Holden, P.; van Achterbergh, E. Microinclusions in monocrystalline octahedral diamonds and coated diamonds from Diavik, Slave Craton: Clues to diamond genesis. *Lithos* **2009**, *112*, 724–735. [[CrossRef](#)]
51. Haggerty, S.E.; Boyd, F.R. Kimberlite inclusions in an olivine megacryst from Monastery. In Proceedings of the De Beers Kimberlite Symposium I, Cambridge, UK, 1975.
52. Jakob, W.R.O. *Geochemical Aspects of the Megacryst Suite from the Monastery Kimberlite Pipe*; University of Cape Town: Cape Town, South Africa, 1977.
53. Pivin, M.; Féménias, O.; Demaiffe, D. Metasomatic mantle origin for Mbuji-Mayi and Kundelungu garnet and clinopyroxene megacrysts (Democratic Republic of Congo). *Lithos* **2009**, *112*, 951–960. [[CrossRef](#)]
54. Kargin, A.V.; Sazonova, L.V.; Nosova, A.A.; Lebedeva, N.M.; Tretyachenko, V.V.; Abersteiner, A. Cr-rich clinopyroxene megacrysts from the Grib kimberlite, Arkhangelsk province, Russia: Relation to clinopyroxene–phlogopite xenoliths and evidence for mantle metasomatism by kimberlite melts. *Lithos* **2017**, 292–293, 34–48. [[CrossRef](#)]
55. Golovin, A.V.; Sharygin, I.S.; Kamenetsky, V.S.; Korsakov, A.V.; Yaxley, G.M. Alkali-carbonate melts from the base of cratonic lithospheric mantle: Links to kimberlites. *Chem. Geol.* **2018**, *483*, 261–274. [[CrossRef](#)]
56. Brett, R.C.; Russell, J.K.; Andrews, G.D.M.; Jones, T.J. The ascent of kimberlite: Insights from olivine. *Earth Planet. Sci. Lett.* **2015**, *424*, 119–131. [[CrossRef](#)]
57. Gavrilenko, M.; Krawczynski, M.; Ruprecht, P.; Li, W.; Catalano, J.G. The quench control of water estimates in convergent margin magmas. *Am. Mineral.* **2019**, *104*, 936–948. [[CrossRef](#)]
58. Horat, K.; Simmons, G. Thermal Conductivity of Rock-Forming Minerals. *Earth Planet. Sci. Lett.* **1969**, *6*, 359–368.
59. Fulop, A.; Kopylova, M.; Kurszlaukis, S.; Hilchie, L.; Ellemers, P.; Squibb, C. Petrography of Snap Lake Kimberlite Dyke (Northwest Territories, Canada) and its Interaction with Country Rock Granitoids. *J. Petrol.* **2018**, *59*, 2493–2518. [[CrossRef](#)]
60. Fulop, A.; Kopylova, M.; Kurszlaukis, S.; Hilchie, L.; Ellemers, P. A Reply to the Comment by Gernon et al. on the Petrography of the Snap Lake Kimberlite Dyke (Northwest Territories, Canada) and its Interaction with Country Rock Granitoids' by Fulop et al. (2018). *J. Petrol.* **2018**, *60*, 661–671. [[CrossRef](#)]
61. Gernon, T.M.; Sparks, R.S.J.; Field, M.; Ogilvie-Harris, R.; Schumacher, J.C.; Brooker, R. Comment on: Petrography of the Snap Lake Kimberlite Dyke (Northwest Territories, Canada) and its Interaction with Country Rock Granitoids'. *J. Petrol.* **2019**, *60*, 649–659.

62. Willcox, A.; Buisman, I.; Sparks, R.S.J.; Brown, R.J.; Manya, S.; Schumacher, J.C.; Tuffen, H. Petrology, geochemistry and low-temperature alteration of lavas and pyroclastic rocks of the kimberlitic Igwisi Hills volcanoes, Tanzania. *Chem. Geol.* **2015**, *405*, 82–101. [[CrossRef](#)]
63. Soltys, A.; Giuliani, A.; Phillips, D.; Kamenetsky, V.S.; Maas, R.; Woodhead, J.; Rodemann, T. In-situ assimilation of mantle minerals by kimberlitic magmas -Direct evidence from a garnet wehrlite xenolith entrained in the Bultfontein kimberlite (Kimberley, South Africa). *Lithos* **2016**, *256–257*, 182–196. [[CrossRef](#)]
64. Klemme, S.; Stalder, R. Halogens in the Earth's Mantle: What We Know and What We Don't. In *The Role of Halogens in Terrestrial and Extraterrestrial Geochemical Processes: Surface, Crust, and Mantle*; Harlov, D.E., Aranovich, L., Eds.; Springer International Publishing: Cham, Switzerland, 2018; pp. 847–869. ISBN 978-3-319-61667-4.
65. Eccles, D.R.; Heaman, L.M.; Luth, R.W.; Creaser, R.A. Petrogenesis of the Late Cretaceous northern Alberta kimberlite province. *Lithos* **2004**, *76*, 435–459. [[CrossRef](#)]
66. Armstrong, J.P.; Wilson, M.; Barnett, R.L.; Nowicki, T.; Kjarsgaard, B.A. Mineralogy of primary carbonate-bearing hypabyssal kimberlite, Lac de Gras, Slave Province, Northwest Territories, Canada. *Lithos* **2004**, *76*, 415–433. [[CrossRef](#)]
67. Kopylova, M.G.; Mogg, T.; Smith, B.S. Mineralogy of the Snap Lake kimberlite, Northwest Territories, Canada, and compositions of phlogopite as records of its crystallization. *Can. Mineral.* **2010**, *48*, 549–570. [[CrossRef](#)]
68. Menzies, A.; Westerlund, K.; Grütter, H.; Gurney, J.; Carlson, J.; Fung, A.; Nowicki, T. Peridotitic mantle xenoliths from kimberlites on the Ekati Diamond Mine property, N.W.T., Canada: Major element compositions and implications for the lithosphere beneath the central Slave craton. *Lithos* **2004**, *77*, 395–412. [[CrossRef](#)]
69. McDonough, W.F.; Sun, S. The composition of the Earth. *Chem. Geol.* **1995**, *120*, 223–253. [[CrossRef](#)]
70. Tappe, S.; Graham Pearson, D.; Kjarsgaard, B.A.; Nowell, G.; Dowall, D. Mantle transition zone input to kimberlite magmatism near a subduction zone: Origin of anomalous Nd-Hf isotope systematics at Lac de Gras, Canada. *Earth Planet. Sci. Lett.* **2013**, *371–372*, 235–251. [[CrossRef](#)]
71. Creaser, R.A.; Grütter, H.; Carlson, J.; Crawford, B. Macrocrystal phlogopite Rb–Sr dates for the Ekati property kimberlites, Slave Province, Canada: Evidence for multiple intrusive episodes in the Paleocene and Eocene. *Lithos* **2004**, *76*, 399–414. [[CrossRef](#)]
72. Nimis, P.; Taylor, W.R. Single clinopyroxene thermobarometry for garnet peridotites. Part I. Calibration and testing of a Cr-in-Cpx barometer and an enstatite-in-Cpx thermometer. *Contrib. to Mineral. Petrol.* **2000**, *139*, 541–554. [[CrossRef](#)]
73. Grütter, H.S. Pyroxene xenocryst geotherms: Techniques and application. *Lithos* **2009**, *112*, 1167–1178. [[CrossRef](#)]
74. Dalton, J.; Presnall, D. Carbonatitic melts along the solidus of model lherzolite in the system CaO–MgO–Al₂O₃–SiO₂–CO₂ from 3 to 7 GPa. *Contrib. Mineral. Petrol.* **1998**, *131*, 123–135. [[CrossRef](#)]
75. Sun, C.; Dasgupta, R. Slab–mantle interaction, carbon transport, and kimberlite generation in the deep upper mantle. *Earth Planet. Sci. Lett.* **2019**, *506*, 38–52. [[CrossRef](#)]
76. Stone, R.S.; Luth, R.W. Orthopyroxene survival in deep carbonatite melts: Implications for kimberlites. *Contrib. to Mineral. Petrol.* **2016**, *171*, 63. [[CrossRef](#)]
77. Sharygin, I.S.; Litasov, K.D.; Shatskiy, A.; Safonov, O.G.; Golovin, A.V.; Ohtani, E.; Pokhilenko, N.P. Experimental constraints on orthopyroxene dissolution in alkali-carbonate melts in the lithospheric mantle: Implications for kimberlite melt composition and magma ascent. *Chem. Geol.* **2017**, *455*, 44–56. [[CrossRef](#)]
78. Kamenetsky, V.S.; Yaxley, G.M. Carbonate-silicate liquid immiscibility in the mantle propels kimberlite magma ascent. *Geochim. Cosmochim. Acta* **2015**, *158*, 48–56. [[CrossRef](#)]
79. Sharygin, I.S.; Litasov, K.D.; Shatskiy, A.; Golovin, A.V.; Ohtani, E.; Pokhilenko, N.P. Melting phase relations of the Udachnaya-East Group-I kimberlite at 3.0–6.5 GPa: Experimental evidence for alkali-carbonatite composition of primary kimberlite melts and implications for mantle plumes. *Gondwana Res.* **2015**, *28*, 1391–1414. [[CrossRef](#)]
80. Shatskiy, A.; Litasov, K.D.; Sharygin, I.S.; Ohtani, E. Composition of primary kimberlite melt in a garnet lherzolite mantle source: Constraints from melting phase relations in anhydrous Udachnaya-East kimberlite with variable CO₂ content at 6.5 GPa. *Gondwana Res.* **2017**, *45*, 208–227. [[CrossRef](#)]
81. Canil, D.; Fedortchouk, Y. Garnet dissolution and the emplacement of kimberlites. *Earth Planet. Sci. Lett.* **1999**, *167*, 227–237. [[CrossRef](#)]

82. Soltys, A.; Giuliani, A.; Phillips, D. Crystallisation sequence and magma evolution of the De Beers dyke (Kimberley, South Africa). *Mineral. Petrol.* **2018**, *112*, 503–518. [[CrossRef](#)]
83. Navon, O.; Hutcheon, I.; Rossman, G.; Wasserburg, G. Mantle-derived fluids in diamond micro-inclusions. *Nature* **1988**, *335*, 784–789. [[CrossRef](#)]
84. Zedgenizov, D.A.; Kagi, H.; Shatsky, V.S.; Sobolev, N.V. Carbonatitic melts in cuboid diamonds from Udachnaya kimberlite pipe (Yakutia): Evidence from vibrational spectroscopy. *Mineral. Mag.* **2004**, *68*, 61–73. [[CrossRef](#)]
85. Izraeli, E.S.; Harris, W.; Navon, O. Brine inclusions in diamonds: A new upper mantle fluid. *Earth Planet. Sci. Lett.* **2001**, *187*, 323–332. [[CrossRef](#)]



© 2019 by the author. Licensee MDPI, Basel, Switzerland. This article is an open access article distributed under the terms and conditions of the Creative Commons Attribution (CC BY) license (<http://creativecommons.org/licenses/by/4.0/>).